Dissociation of the Single-Ring Chaperonin GroEL by High Hydrostatic Pressure†

Markandeswar Panda, Jesse Ybarra, and Paul M. Horowitz*

Department of Biochemistry, Mail Code 7760, University of Texas Health Science Center at San Antonio, 7703 Floyd Curl Drive, San Antonio, Texas 78229-3900

Received May 16, 2002

ABSTRACT: We investigated the dissociation of single-ring heptameric GroEL (SR1) by high hydrostatic pressure in the range of 1−2.5 kbar. The kinetics of the dissociation of SR1 in the absence and presence of Mg^{2+}, KCl, and nucleotides were monitored using light scattering. The major aim of this investigation was to understand the role of the double-ring structure of GroEL by comparing its dissociation with the dissociation of the single ring. At all the pressures that were studied, SR1 dissociates much faster than the GroEL 14mer. As observed with the GroEL 14mer, SR1 also showed biphasic kinetics and the dissociated monomers do not reassociate readily back to the oligomer. Unlike the GroEL 14mer, the observed rates for SR1 dissociation are independent of the concentrations of Mg^{2+} and KCl in the studied range. The effects of nucleotides on the observed rates, in the absence or presence of Mg^{2+} and KCl, are not very significant. The heterogeneity induced in the GroEL molecule with the double-ring structure by ligands such as Mg^{2+}, KCl, and nucleotides is not observed in the case of SR1. This indicates that the inter-ring negative cooperativity in the double-ring GroEL has a major role in this regard. The results presented in this investigation demonstrate that the presence of a second ring in the GroEL 14mer is important for its stability in an environment where the functional ligands of the chaperonin are available.

From high-pressure studies, it has been known that at pressures above 3−4 kbar[1] many proteins could be denatured (*1*−*3*). At pressures below 3 kbar, oligomeric proteins or protein assemblies generally undergo reversible dissociation into subunits (*3*, *4*). High-hydrostatic pressure techniques have been used in studying dissociation of oligomeric proteins and protein aggregates and unfolding of monomeric proteins (*2*, *4*−*15*) in the absence of externally added chaotropes. The important theories behind this technique and excellent experimental details can be found in several edited books and monographs (*2*, *16*−*21*). In a recent review, Silva et al. (*22*) have discussed many important aspects of high pressure, providing new insights into the folding and dynamics of proteins. A brief summary of the physical forces responsible for the dissociation of oligomers by high hydrostatic pressure can be found in our earlier work on GroEL dissociation (*23*).

In the past few years, we have been using the bacterial chaperonin GroEL as a model for studying the effect of high hydrostatic pressure on the dissociation of macromolecular assemblies (*23*−*25*). GroEL and its co-chaperonin GroES are multimeric proteins that assist in the folding of other proteins by preventing misfolding and aggregation. Both of these chaperonins are essential for protein folding *in vivo* (*26*−*28*). GroEL is a tetradecamer (14mer) of 57 kDa subunits arranged in two, seven-membered rings stacked back to back to yield a cylindrical structure (*29*−*32*). The X-ray crystal structures of GroEL (*29*, *30*), GroEL fully complexed with 14 ATPγS molecules (*31*), and the GroEL−GroES−$(ADP)_7$ complex (*32*) are available. There are no tryptophan residues, and each subunit contains three cysteines: Cys138, Cys458, and Cys519. The crystal structure demonstrates that each monomer (547 amino acids) is folded into three distinct domains, e.g., apical, equatorial, and intermediate domains. The apical domain faces the solvent, forms the opening to the central channel, and contains the GroES and peptide binding site. The highly helical equatorial domain contains the ATP binding site and forms the inter- and intraring contacts of the double ring of the GroEL 14mer. The hingelike intermediate domain links the apical and equatorial domains and transfers the ATP-induced conformational changes between the equatorial and the apical domain (*29*, *32*). Briefly, the GroEL-assisted protein folding reaction cycle consists of a number of sequential reactions such as the binding of the polypeptide at the apical domains of the cis ring, binding of seven molecules of ATP and GroES, forming a stable cis assembly and freeing the tightly bound polypeptide into an enclosed space where it folds with hydrolysis of ATP, followed by the release of ADP, GroES, and the folded polypeptide (*32*−*37*). The presence of Mg^{2+} and K^+ is also necessary for the GroEL-assisted folding cycle (*38*−*42*). ATP plays an important role both as an energy source and as an allosteric effector, and its binding displays both intraring positive cooperativity and inter-ring negative cooperativity (*43*−*45*). The role of Mg^{2+} as a structural ligand is important for the GroEL−GroES system (*38*−*42*).

† This research was supported by National Institutes of Health Grant NIHGM25177 and Robert A. Welch Foundation Grant AQ723 (to P.M.H.).

* To whom correspondence should be addressed. Telephone: (210) 567-3737. Fax: (210) 567-6595. E-mail: horowitz@biochem.uthscsa.edu.

[1] Units of pressure: 1 bar = 0.1 Mpa (megapascal) = 0.987 atm = 14.5 psi (pounds per square inch); 1 kbar = 1000 bar. Abbreviations: ATP, adenosine 5′-triphosphate; ADP, adenosine 5′-diphosphate; AMP, adenosine 5′-monophosphate; AMP-PNP, adenosine 5′-(β,γ-imido)-triphosphate; ATPγS, adenosine 5′-*O*-(3-thiotriphosphate).

10.1021/bi020366j CCC: $22.00
Published on Web 09/26/2002

We have reported that high hydrostatic pressure can dissociate GroEL tetradecamers (*46*). After depressurization, the monomers reassociated back to the oligomer only very slowly with a $t_{1/2}$ of 150 h at 25 °C. The dissociation and association reactions were facilitated by MgATP only if it was present during pressurization. Recently, we have shown that high hydrostatic pressure can probe the effects of functionally related ligands (Mg^{2+} and adenine nucleotides) on GroEL, GroES, and the GroEL−GroES−$(ADP)_7$ complex (*23*). Similarly, we have provided evidence for the presence of conformational heterogeneity in the native GroEL 14mer (*25*). The evidence for this heterogeneity was obtained from the observation that the 14mers dissociated to a mixture of monomers and undissociated 14mers depending upon an applied pressure of <2.5 kbar (*23*). This was evident from both the amplitudes of the reactions at the end of the kinetics and subsequent native gel analyses of the products. From the effect of the concentrations of Mg^{2+}, KCl, and nucleotides on the dissociation rates, we concluded that the binding of these functionally related ligands with the GroEL 14mer imparts different stabilities to the chaperonin (*23*−*25*). During the isolation and purification of GroEL, several reagents such as Mg^{2+} and KCl are added and it is possible that such binding might produce heterogeneous populations of GroEL bound by these reagents (*25*).

In view of the observations described above, there have been studies aimed at understanding the role played by the individual heptameric rings of the double-ring (14mer) GroEL. The mutation of four residues (R452E, E461A, S463A, and V464A) that prevent the major contacts between the two rings of GroEL produces the single-ring mutant termed SR1 (*47*, *48*). Using gel filtration and electron microscopy, Weissman et al. (*47*) have shown the structure was a single ring. Recently, Holzinger et al. have used small-angle neutron scattering to support the single-ring structure of SR1 (*49*). Many interesting results are observed with SR1. (i) In the presence of ATP, it could bind but not readily release GroES (*47*). (ii) The single rings do not associate to double rings in the presence of GroES and ATP (*50*). (iii) In the presence of GroES, ATP or ADP, and 80 mM KCl, it supports the folding of rhodanese (*51*). (iv) Inter-ring negative cooperativity in the double ring GroEL is important (*52*, *53*). Therefore, we conducted the investigation presented here to compare the dissociation induced by high hydrostatic pressures of single-ring versus double-ring GroEL chaperonin. As the results show, the single ring does not have the ability to induce stablity in the heptameric ring in the presence of the functional ligands or the characteristic native state heterogeneity shown by the double-ring GroEL attributed to ligand binding.

MATERIALS AND METHODS

SR1-GroEL was purified from lysates of *Escherichia coli* cells bearing the multicopy plasmid pHOG1-SR1 (a gift from C. Frieden, Washington University School of Medicine, St. Louis, MO). The construction of pHOG1-SR1 from the site-directed mutagenesis of pHOG1 with mutations R452E, E461A, S463A, and V464A has been reported previously (*54*). The fluorescent contaminants from the isolated GroEL were removed by eluting the protein from a Reactive Red 120 agarose (type 3000-CL) column equilibrated with 50 mM Tris-HCl buffer (pH 7.5), 5 mM Mg^{2+}, and 0.5 mM DTT at 4 °C (*54*). The final preparation gave single bands by both native and denaturing gel electrophoresis.

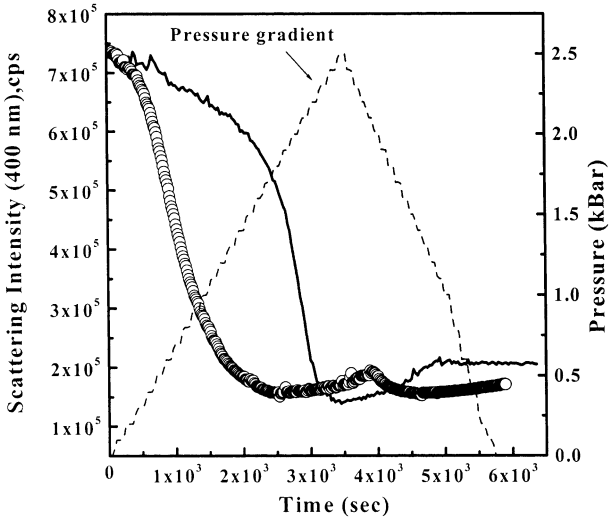

FIGURE 1: Dissociation plots for SR1 (○) and GroEL-14 mer (—) in a pressure gradient from 0.1 to 2.5 kbar and from 2.5 to 0.1 kbar. Both the light scattering intensities (left ordinate) vs time and pressure (right ordinate) vs time data were collected at 15 s intervals, using two independent computers. The pressure was increased by 0.1 kbar units until it reached 2.5 kbar and then decreased in the same intervals (- - -). At each 0.1 kbar interval, the corresponding pressure was maintained for 1 min. Light scattering was monitored at 400 nm. The dissociation pattern of the GroEL 14mer (—) is from ref *23* and is shown for comparison between the two proteins. Further experimental details can be found in Materials and Methods. The reaction conditions were as follows: 1.43 μM SR1, 0.36 μM GroEL 14mer, 50 mM Tris, pH 7.8, and 25 °C.

The buffer solutions used in the kinetics experiments were filtered through 0.2 μm surfactant free cellulose acetate membrane syringe filters (Nalgene). Tris buffer was used because of its small pK_a dependence upon hydrostatic pressure (*55*).

High-Pressure Experiments. The high-pressure generator was from Advanced Pressure Products (APP, Ithaca, NY). The high-pressure cell and photon counting spectrofluorometer were from ISS Inc. (Champaign, IL). The stainless steel alloy cell with quartz windows can be pressurized up to 3 kbar. Protein samples for the experiments were contained in quartz bottles (1 mL volume) with pressure caps (provided by ISS). Spectroscopic-grade ethanol was used as the pressurizing fluid. The pressure generator was electronically controlled and could be programed to obtain pressure gradients. The temperature of the high-pressure cell was maintained by a circulating water bath. Two independent computers controlled the APP pressure generator and ISS spectrofluorometer. A program written for the APP software controlled the target pressure. Experiments where a pressure gradient was applied (e.g., Figure 1) were carried out using a program written for the APP software. The pressure was increased in 0.1 kbar increments and held for 1 min between successive steps. The generated data were imported into Origin software (version 6, Microcal Software, Northampton, MA) and analyzed. Kinetics experiments were carried out by first equilibrating the protein sample in the pressure cell for 1 h at the desired temperature. After equilibration, the fluorometer recording was turned on, followed by the pressure machine. Light scattering at 400 nm was used to monitor the dissociation process of SR1. The excitation and

emission slits were 2 (16 nm band-pass) and 1 mm (8 nm band-pass), respectively. In typical experiments, to reach pressures of 1 kbar required 1 min, 2 kbar required 3 min, and 2.5 kbar required 4.5 min at a pump speed of 2.0. The limitations and reasons to avoid fast pressurization and depressurization have been discussed in our earlier work (*23*). In general, rapid pressure changes cause damage by shattering the quartz windows or sample bottles. Control experiments using latex beads have shown that the intensity changes were not contributed by dimension changes of the cell due to high pressure (*23*).

Analysis of Kinetics Data. The data were truncated to take into account the time taken by the pressure cell to reach the target pressure. The rates were evaluated by fitting the data to either mono- or biexponential equations: $Y = A_1 \times \exp(-k_1 t) + A_2$ or $Y = A_1 \times \exp(-k_1 t) + A_2 \times \exp(-k_2 t) + A_3$, respectively. The independent variable Y was the observed scattering intensity in counts per second (cps) after subtraction of the scattering due to buffer. The pseudo-first-order rate constants k_1 and k_2 and the parameters relating the amplitudes A_1-A_3 were obtained from iterative nonlinear least-squares regression of the data using the Origin software program (MicroCal).

RESULTS AND DISCUSSION

The kinetics of the dissociation of SR1 (single-ring GroEL) at pressures in the range of 0.5−3 kbar were studied for ~10 half-lives at 25 °C in 50 mM Tris-HCl buffer (pH 7.8). A comparison of the dissociation processes of the GroEL 14mer (double ring) and this single-ring mutant under the pressure gradient is shown in Figure 1. As can be seen, the SR1 mutant dissociates much faster than the GroEL 14mer at each of the applied pressures. The final scattering intensities are consistent with the dissociation going completely to monomers. This has been verified by native gel electrophoresis of the products at the end of the pressure dissociation experiments. In the curves shown in Figure 1, each data point represents the observed light scattering intensity at a specific pressure that was maintained for an interval of 1 min. During these intervals, there are pressure-dependent kinetics. Hence, it is not possible to fit such data to obtain any useful parameters. Therefore, for the sake of comparison, the apparent $p_{1/2}$ values (the pressure at which the dissociation process shows one-half of the total intensity change) can be compared. These $p_{1/2}$ values are 0.7 kbar for SR1 and 1.45 kbar for the GroEL 14mer. The typical kinetics followed by light scattering at 400 nm and their biexponential fits at 2.0 kbar are shown in Figure 2. The kinetic trace in the case of SR1 was fitted to the biexponential rate equation (see Materials and Methods) and yields a $k_{1,obs}$ of $(1.24 \pm 0.02) \times 10^{-2}$ s^{-1} and a $k_{2,obs}$ of $(8.30 \pm 0.10) \times 10^{-4}$ s^{-1} for SR1 and a single monophasic reaction with a $k_{1,obs}$ of $(4.60 \pm 0.05) \times 10^{-4}$ s^{-1} in the case of the GroEL 14mer.

The results from pressurization and depressurization of SR1 are shown in Figure 3. SR1 in the presence of 1 mM ATP, 5 mM Mg^{2+}, 10 mM KCl, and 50 mM Tris (pH 7.8) at 25 °C was dissociated at 2.0 kbar (see the legend of Figure 3). In panel A, the kinetics are shown along with the point (shown by an arrow) where the system was depressurized to 1 bar. The light scattering intensity was monitored to observe any increase in the magnitude due to reassociation.

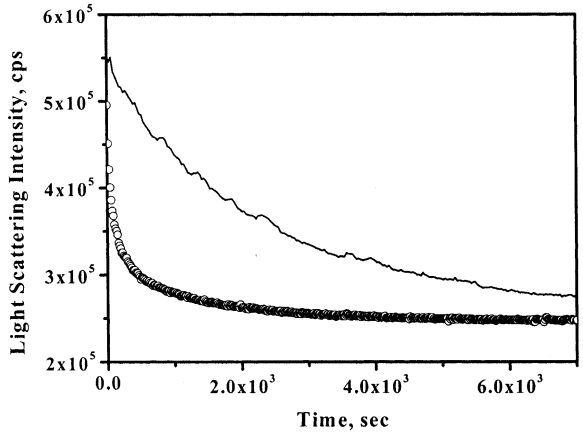

FIGURE 2: Effect of pressure on the kinetics of dissociation of SR1 and the GroEL 14mer. SR1 and GroEL were dissociated at 2 kbar as described in Materials and Methods, and the kinetics were monitored using scattering at 400 nm (excitation and emission) until the reactions reached plateaus. For the sake of clarity, only parts of the complete kinetics (followed for 10 half-lives) are shown. The solid line through the data (○) is a fit to the data using a biexponential equation (see Materials and Methods). The observed rates from biexponential fits (see Materials and Methods) of the data were a $k_{1,obs}$ of $(1.24 \pm 0.02) \times 10^{-2}$ s^{-1} and a $k_{2,obs}$ of $(8.30 \pm 0.10) \times 10^{-4}$ s^{-1} for SR1 and a single monophasic reaction with a $k_{1,obs}$ of $(4.60 \pm 0.05) \times 10^{-4}$ s^{-1} in the case of the GroEL 14mer (see Results and Discussion). The reaction conditions were as follows: 1.43 μM SR1, 0.36 μM GroEL 14mer, 50 mM Tris, pH 7.8, and 25 °C. Other details such as conditions for monitoring the kinetics and the pressure setup are in Materials and Methods.

It is evident from panel B that the increase is either too slow or insignificant within the time period that was studied. Similar experiments were carried out in the presence or absence of nucleotides, Mg^{2+}, and KCl. There were not any observable scattering intensity changes after depressurization for 18−20 h in any of the cases. This demonstrates that the dissociation of SR1 leading to monomers occurs in a nonreversible path. Similar observations have been noted in our earlier work on GroEL 14mer dissociation by hydrostatic pressure, where the monomers did not reassociate readily upon depressurization (*23*). Monitoring the bis-ANS fluorescence, Gorovits et al. had shown that the reassociation of monomers from GroEL 14mer dissociation was extremely slow with a $t_{1/2}$ of 150 h at 25 °C (*24*). In the investigation presented here, we were unable to detect any reassociated 7mer even after storing the dissociated monomers for 1 month from any of the reaction conditions shown in Table 1. This confirms our earlier hypothesis that the dissociated monomers undergo conformational drift, making them unsuitable for reassociation (*23*, *25*), and this also happened when the oligomer was a single-ring mutant instead of a double ring. It is important to note that the conformational drift of the monomers is different from the conformational heterogeneity observed in the case of the GroEL 14mer. The former refers to the pressure deformation of the monomers that makes them unable to reassemble to oligomers upon depressurization, whereas the latter is the relative stability with respect to its dissociation at a definite pressure when the oligomer is bound to a functionally related ligand (*23*, *25*). At present, we have been unable to find a technique such as gel filtration or circular dichroism to distinguish between the conformations of the monomers generated by chaotropes and high pressure. The only properties known

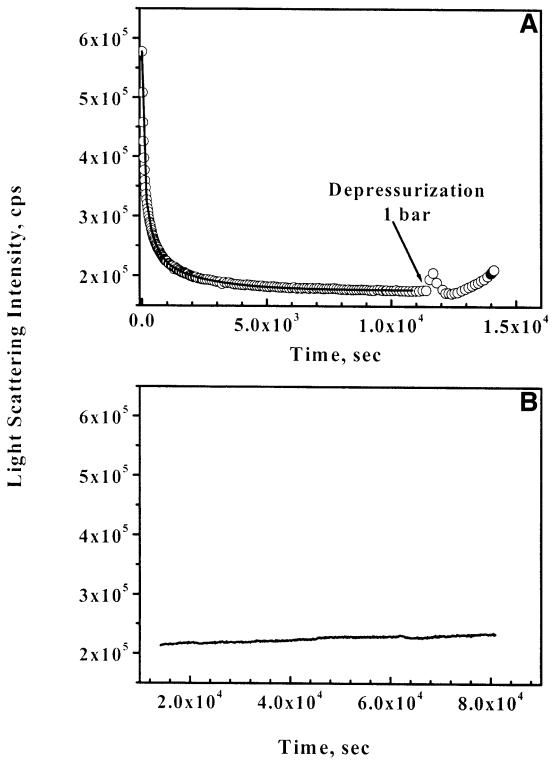

FIGURE 3: Effects of repressurization and depressurization on the light scattering intensity of SR1. Dissociation kinetics were followed as described in Materials and Methods. The reaction conditions were as follows: 1.43 μM SR1, 1.0 mM ATP, 5 mM Mg^{2+}, 10 mM KCl, 50 mM Tris, pH 7.8, and 25 °C. The reaction profiles shown in the two panels (A and B) are using the same sample of SR1 in the pressure cuvette, and with identical setups of the instrument parameters except the applied pressures as discussed. All the times presented on the abscissa of the panels are continuous with the initial zero at the beginning of panel A. The reaction was monitored for 190 min at 2.00 kbar, which followed biexponential kinetics (A) and depressurized to 1 bar. After a few minutes, the recording was continued at 2 min intervals for ~20 h (B), where there is only a very minor increase in the scattering intensity compared to the major decrease observed in panel A.

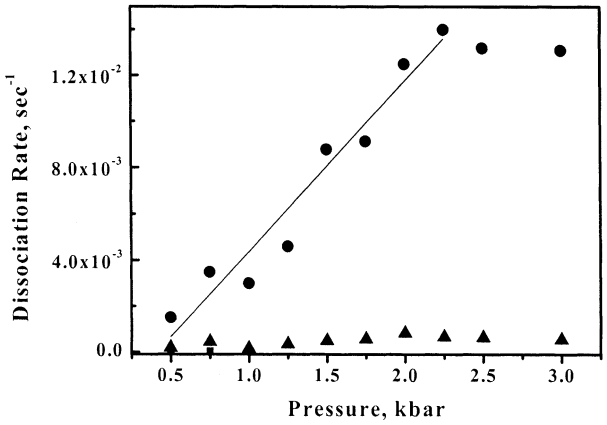

FIGURE 4: Effect of pressure on the observed dissociation rates of SR1. The observed dissociation rates of SR1 at different presuures in the range of 0.5−3.00 kbar were obtained from the biphasic fits to the light scattering kinetics. The faster rates ($k_{1,obs}$) are represented by filled circles, and the slower rates ($k_{2,obs}$) are represented by filled traingles. In a few cases at the very low pressures (0.5−1.0 kbar), the kinetics fitted well to three phases and the third slow phase is shown as filled squares (see Results and Discussion). This faster phase ($k_{1,obs}$) has ~80% of the total amplitude of the dissociation reaction. The slower phase ($k_{2,obs}$) at any specific pressure that was studied was ~12−15 times slower than the corresponding fast phase and was independent of pressure. The reaction conditions were as follows: 1.43 μM SR1, 50 mM Tris, pH 7.8, and 25 °C. Other conditions for monitoring the kinetics and pressure setup are in Materials and Methods.

so far are that monomers generated by urea dissociation of the GroEL 14mer could be reassembled back to oligomers upon removal or dilution of urea in the presence of Mg^{2+}, ATP or ADP, and $(NH_4)_2SO_4$ (*56*), whereas monomers formed by high pressure from the GroEL 14mer (*23*) or SR1 in the investigation presented here do not reassemble under similar conditions.

The kinetics of dissociation of SR1 at different applied pressures were studied in the range of 0.5−3.0 kbar under identical reaction conditions (see the legend of Figure 4) in the absence of nucleotides, Mg^{2+}, or KCl. The results are presented in Figure 4. All the kinetics fitted to a biexponential equation (see Materials and Methods) except at pressures of <1 kbar where they fitted to a three-exponential rate equation. However, the second and third observed rates were nearly identical in magnitude. In Figure 4, the faster rate ($k_{1,obs}$) increased with pressure until 2 kbar, after which it reached a plateau (●). The slower rates [both $k_{2,obs}$ (▲) and $k_{3,obs}$ (■)] are independent of the applied pressure. In the case of the GroEL 14mer, the dissociation exhibited biexponential kinetics below 1.75 kbar and monoexponential kinetics above 1.75 kbar; the amplitudes of both the fast and slow phases decreased with the decrease in applied pressure (*23*). In general, for the GroEL 14mer, the observed rates of the fast ($k_{1,obs}$, major phase) process increased slowly until 2 kbar, and then increased rapidly after that (*23*) until 3 kbar without any observable plateau. In contrast to this, all the kinetic traces for SR1 in the study presented here at these pressures provide identical amplitudes, and the analysis of products on a native gel shows complete dissociation into monomers except at the very low pressure of 0.5 kbar. The native gel for the dissociated products from the GroEL 14mer had shown the presence of different amounts of oligomers and monomers until 2 kbar (*23*), which along with other evidences was attributed to the presence of heterogeneity in the native GroEL 14mer (*25*). Therefore, these results for SR1 are completely different from those observed earlier for GroEL 14mer dissociation at different pressures (*23*, *25*), and SR1 does not contain detectable heterogeneity in the native state.

The observed rates ($k_{1,obs}$ and $k_{2,obs}$) obtained from the biexponential fits to the kinetics for the dissociation of SR1 at 2 kbar, where the Mg^{2+} concentration was varied, are shown in Figure 5. It may be noted that the variation of the Mg^{2+} concentration in this investigation was studied at 2 kbar instead of at 2.5 kbar for the 14mer reported previously (*23*, *25*) since the dissociation of SR1 reaches a maximum at 2 kbar. A pressure of 2.5 kbar was used for the GroEL 14mer since at that pressure the dissociation led to 100% monomers. It is clear from the results in Figure 5 that both the slow and fast rates are unaffected by the added Mg^{2+} concentration in the range that was studied (0−10 mM). In the case of the 14mer, the dependencies of both rates were dramatic, where the rates decreased exponentially with an increase in Mg^{2+} concentration and reached a minimum around 3 mM $MgCl_2$ (*25*). Therefore, the effect of Mg^{2+} is clearly responsible for the inter-ring interactions of the

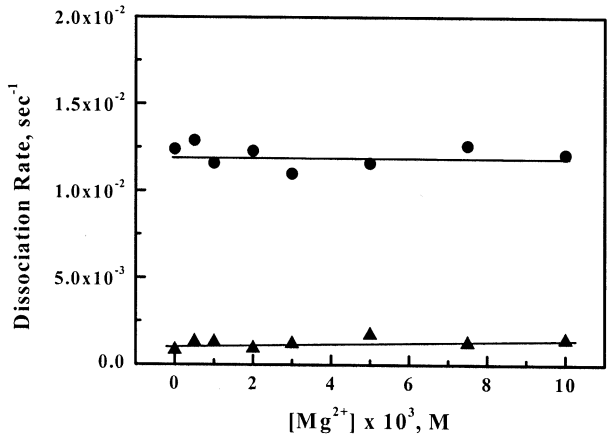

FIGURE 5: Effect of added Mg^{2+} on the dissociation rate of SR1 at 2.0 kbar. The observed fast [$k_{1,obs}$ (●)] and slow [$k_{2,obs}$ (▲)] rates obtained from biexponential fits as a function of added Mg^{2+} concentration. The lines drawn through the data are only for the purpose of visualizing the data. The reaction conditions were as follows: 1.43 μM SR1, 50 mM Tris, pH 7.8, and 25 °C.

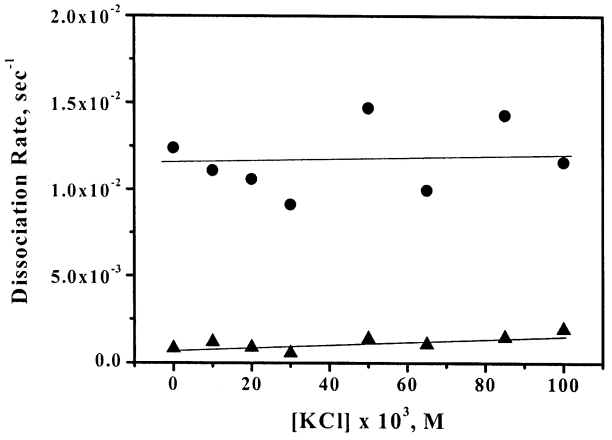

FIGURE 6: Effect of added KCl on the dissociation rate of SR1 at 2.0 kbar. The observed fast [$k_{1,obs}$ (●)] and slow [$k_{2,obs}$ (▲)] rates obtained from biexponential fits vs KCl concentration. The lines drawn through the data are only for the purpose of visualizing the data. The reaction conditions were as follows: 1.43 μM GroEL, 50 mM Tris, pH 7.8, and 25 °C.

GroEL 14mer containing the double ring and does not have any effect on the intraring positive cooperativity present in the individual heptameric rings.

The independence of the observed rates for the dissociation of SR1 at 2 kbar, as a function of KCl concentration in the range of 0−100 mM, is shown in Figure 6. This is entirely different from the earlier report on the dissociation of the GroEL 14mer. At 2.5 kbar, the dissociation rates (both $k_{1,obs}$ and $k_{2,obs}$) of the 14mer show smooth exponential decreases with the increase in the KCl concentration, reaching minima at high concentrations of added KCl (*25*). The results were rationalized on the basis of the hypothesis that KCl imparts some tightness by the formation of salt bridges that are broken in a kinetically controlled process, leading to slower observed rates as the concentration of this reagent was increased (*25*). From the independence of the observed SR1 dissociation rates on KCl concentration, it appears that such salt bridges are important only for the double ring and therefore important in the inter-ring interactions of GroEL.

The effects of adenine nucleotides such as ATP, ADP, AMP, AMP-PNP, and ATPγS both in the absence and presence of Mg^{2+} and KCl on the dissociation of SR1 at 2 kbar were studied. These results are collected in Table 1. The process leading to the faster rate ($k_{1,obs}$) always consisted of the major amplitude in all cases. However, the effects are not dramatic as seen from the comparison of the rates

Table 1: Kinetics of Dissociation of SR1-GroEL as a Function of Added Reagents at 2 kbar[a]

	fast phase		slower phase	
reagent	k_1 (s^{-1})	% amplitude (A_1)	k_2 (s^{-1})	% amplitude (A_2)
buffer only	$(1.24 \pm 0.02) \times 10^{-2}$	68	$(8.30 \pm 0.10) \times 10^{-4}$	32
5 mM Mg^{2+}	$(1.16 \pm 0.03) \times 10^{-2}$	63	$(1.74 \pm 0.04) \times 10^{-3}$	37
10 mM KCl	$(1.10 \pm 0.03) \times 10^{-2}$	66	$(1.20 \pm 0.03) \times 10^{-3}$	34
10 mM potassium glutamate	$(1.55 \pm 0.05) \times 10^{-2}$	60	$(9.80 \pm 0.20) \times 10^{-4}$	40
5 mM Mg^{2+} and 10 mM KCl	$(1.11 \pm 0.02) \times 10^{-2}$	69	$(1.19 \pm 0.02) \times 10^{-3}$	31
1 mM ATP	$(1.50 \pm 0.05) \times 10^{-2}$	75	$(8.60 \pm 0.30) \times 10^{-4}$	25
1 mM ATP and 5 mM Mg^{2+}	$(9.91 \pm 0.10) \times 10^{-3}$	77	$(1.00 \pm 0.01) \times 10^{-3}$	23
1 mM ATP, 5 mM Mg^{2+}, and 10 mM KCl	$(9.55 \pm 0.16) \times 10^{-3}$	70	$(8.40 \pm 0.10) \times 10^{-4}$	30
1 mM ADP	$(1.61 \pm 0.04) \times 10^{-2}$	68	$(1.07 \pm 0.02) \times 10^{-3}$	32
1 mM ADP and 5 mM Mg^{2+}	$(1.02 \pm 0.04) \times 10^{-2}$	76	$(9.20 \pm 0.30) \times 10^{-4}$	24
1 mM ADP, 5 mM Mg^{2+}, and 10 mM KCl	$(1.07 \pm 0.02) \times 10^{-2}$	78	$(8.40 \pm 0.20) \times 10^{-4}$	22
1 mM ATPγS	$(1.80 \pm 0.08) \times 10^{-2}$	67	$(1.02 \pm 0.03) \times 10^{-3}$	33
1 mM ATPγS and 5 mM Mg^{2+}	$(6.61 \pm 0.22) \times 10^{-3}$	86	$(4.30 \pm 0.40) \times 10^{-4}$	14
1 mM ATPγS, 5 mM Mg^{2+}, and 10 mM KCl	$(1.19 \pm 0.02) \times 10^{-2}$	78	$(1.00 \pm 0.01) \times 10^{-3}$	22
1 mM AMP	$(7.72 \pm 0.24) \times 10^{-3}$	70	$(6.50 \pm 0.20) \times 10^{-4}$	30
1 mM AMP and 5 mM Mg^{2+}	$(7.78 \pm 0.11) \times 10^{-3}$	72	$(7.70 \pm 0.10) \times 10^{-4}$	28
1 mM AMP, 5 mM Mg^{2+}, and 10 mM KCl	$(7.48 \pm 0.13) \times 10^{-3}$	71	$(7.80 \pm 0.10) \times 10^{-4}$	29
1 mM AMP-PNP	$(1.36 \pm 0.02) \times 10^{-2}$	73	$(1.10 \pm 0.01) \times 10^{-3}$	27
1 mM AMP-PNP and 5 mM Mg^{2+}	$(1.16 \pm 0.02) \times 10^{-2}$	77	$(1.04 \pm 0.02) \times 10^{-3}$	23
1 mM AMP-PNP, 5 mM Mg^{2+}, and 10 mM KCl	$(1.28 \pm 0.02) \times 10^{-2}$	83	$(9.00 \pm 0.20) \times 10^{-4}$	17

[a] The % values are the relative amplitudes of the corresponding phase of the observed biphasic kinetics. The amplitudes for phases corresponding to the observed rates $k_{1,obs}$ and $k_{2,obs}$ refer to A_1 and A_2, respectively, in the biexponential equation (see Materials and Methods). The total amplitude of the reaction is taken to be 100%. Conditions: 50 mM Tris, 1.43 μM SR1, pH 7.8, and 25 °C.

from a reaction in buffer alone. The slowest $k_{1,obs}$ (6.61×10^{-3} s^{-1}) in the presence of 1 mM ATPγS and 5 mM Mg^{2+} is only ~2.7 times slower than the fastest observed dissociation rate (1.80×10^{-2} s^{-1}) in 1 mM ATPγS, whereas this dissociation rate in buffer alone is 1.24×10^{-2} s^{-1}. Similar observations can be drawn for the $k_{2,obs}$ rates in the presence and absence of the nucleotides and ligands. Therefore, it is reasonable to conclude that the dissociation process of the SR1 heptamer was not dramatically different in the presence of these ligands from that in buffer alone. This is a remarkable observation compared to the high-pressure dissociation of the GroEL 14mer, where we reported significant changes in rates due to the addition of these ligands (*23*, *25*).

We studied the effect of potassium glutamate on the pressure dissociation rates of both SR1 and the GroEL 14mer since Cl^- being a chaotrope may counter the stability effect of K^+. The observed rates for SR1 dissociation at 2.0 kbar are included in Table 1. The magnitudes of the observed biphasic rates (k_1 and k_2) in 10 mM potassium glutamate are only slightly higher than those in 10 mM KCl. This clearly shows that these ions do not exert significant changes in the pressure dissociation of SR1. In the case of the GroEL 14mer at 2.5 kbar, the magnitudes of the major phase (k_1) of the observed biphasic rates were $(1.26 \pm 0.06) \times 10^{-3}$ and $(9.60 \pm 0.50) \times 10^{-4}$ s^{-1} in the presence of 10 mM KCl and potassium glutamate, respectively. These two values are not significantly different from each other, although both of them are significantly lower than the observed rate of $(2.86 \pm 0.02) \times 10^{-3}$ s^{-1} (*25*) in Tris buffer alone. Therefore, the effect of Cl^- on the system can be ruled out.

CONCLUSIONS

To understand the importance of the effect of ligands on the intraring positive cooperativity and inter-ring negative cooperativity in the double-ring GroEL, we studied the dissociation of the single-ring mutant (SR1) by high hydrostatic pressure. The results presented in this investigation were compared with those of the dissociation of the GroEL 14mer by high hydrostatic pressure reported previously (*23*, *25*).

The ability of the double-ring GroEL to sequester unfolded peptides and to assist in their proper folding is well-established in the literature. In general, the mechanism involves the action of ATP, Mg^{2+}, and the co-chaperonin GroES for effective folding (*34*, *36*). In the presence of the functional ligands and GroES, GroEL shows allosteric behavior that is attributed to the induced conformational changes in its domains (*32*, *45*, *57*). To understand the inter-ring communication associated with the negative cooperativity and symmetry in the GroEL complex (*36*, *44*, *58*) and the need for the ATP binding to the trans ring to eject the GroES cap as well as the bound peptide, the single-ring mutant was constructed. SR1 in the presence of GroES and ATP has been shown to assist in the folding of rhodanese, malate dehydrogenase, and green fluorescent protein (*48*, *50*). However, the folded polypeptide remains sequestered because of the absence of a second ring preventing the ATP-mediated signaling necessary to release GroES and the peptide (*44*).

Unlike the GroEL 14mer, SR1 undergoes complete dissociation, in a kinetically controlled manner, into monomers in the range of 0.75−3.00 kbar. At the lowest pressure that was studied (0.5 kbar), there were some undissociated 7mers exhibiting incomplete dissociation. In contrast, the extent of dissociation in the case of the GroEL 14mer depends on the applied pressure in addition to the kinetics (*25*). For example, upon native gel analysis of the products after the completion of the kinetics processes, the fraction of undissociated monomers decreased as the applied pressure increased (*23*, *25*). From the study of the effect of Mg^{2+}, KCl, and nucleotides on the dissociation process, it was concluded that these ligands introduced conformational heterogeneity in the GroEL double ring.

From mutational studies on the single-ring and double-ring GroELs, Rye et al. (*59*) have shown that the carboxylate group of aspartate at position 398 directly coordinates with Mg^{2+} and exhibits only ~2% ATP hydrolysis activity. In the study presented here, SR1 contains aspartate 398 and must bind Mg^{2+}. Therefore, the independence of the dissociation rates by high pressure from Mg^{2+} concentration points out to the fact that in the absence of a second ring the binding of this ligand does not induce any stabilization in the 7mer. This is entirely different than the case of the GroEL 14mer, where Mg^{2+} binding induces a relatively stable GroEL (*23*, *25*).

The dissociation rates were completely independent of Mg^{2+} or KCl concentration. Similarly, the observed rates were nearly identical when a combination of Mg^{2+}, KCl, and nucleotides was used (Table 1). This clearly demonstrates that such ligands impart different degrees of stability to GroEL only when both rings of the chaperonin are present.

REFERENCES

1. Paladini, A. A., Jr., and Weber, G. (1981) *Biochemistry 20*, 2587−2593.
2. Weber, G. (1992) *Protein Interactions*, Chapman and Hall, New York.
3. Gross, M., and Jaenicke, R. (1994) *Eur. J. Biochem. 221*, 617−630.
4. Rietveld, A. W., and Ferreira, S. T. (1996) *Biochemistry 35*, 7743−7751.
5. Weber, G. (1993) *J. Phys. Chem. 97*, 7108−7115.
6. Silva, J. L., and Weber, G. (1993) *Annu. Rev. Phys. Chem. 44*, 89−113.
7. Mozhaev, V. V., Heremans, K., Frank, J., Masson, P., and Balny, C. (1996) *Proteins 24*, 81−91.
8. Cioni, P., and Strambini, G. B. (1996) *J. Mol. Biol. 263*, 789−799.
9. Drljaca, A., Hubbard, C. D., van Eldik, R., Asano, T., Basilevsky, M. V., and Le Noble, W. J. (1998) *Chem. Rev. 98*, 2167−2289.
10. Gorovits, B. M., and Horowitz, P. M. (1998) *Biochemistry 37*, 6132−6135.
11. St. John, R. J., Carpenter, J. F., and Randolph, T. W. (1999) *Proc. Natl. Acad. Sci. U.S.A. 96*, 13029−13033.
12. Lassalle, M. W., Yamada, H., and Akasaka, K. (2000) *J. Mol. Biol. 298*, 293−302.
13. Galan, A., Sot, B., Llorca, O., Carrascosa, J. L., Valpuesta, J. M., and Muga, A. (2001) *J. Biol. Chem. 276*, 957−964.
14. Seemann, H., Winter, R., and Royer, C. A. (2001) *J. Mol. Biol. 307*, 1091−1102.
15. Webb, J. N., Webb, S. D., Cleland, J. L., Carpenter, J. F., and Randolph, T. W. (2001) *Proc. Natl. Acad. Sci. U.S.A. 98*, 7259−7264.
16. Sherman, W. F., and Stadtmuller, A. A. (1987) *Experimental Techniques in High-Pressure Research*, Wiley, Chichester, U.K.
17. Jannasch, H. W., Marquis, R. E., and Zimmerman, A. M. (1987) in *Current Perspectives in High-Pressure Biology*, Academic Press, Orlando, FL.

18. van Eldik, R., and Jonas, J. (1987) in *NATO ASI Series (Advanced Scientific Institute) C: Mathematical and Physical Science*, Vol. 197, Reidel, Dordrecht, The Netherlands.
19. Winter, R., and Jonas, J. (1993) in *NATO ASI Series (Advanced Science Institute) C: Mathematical and Physical Science*, Vol. 401, Kluwer Academic Publishers, Dordrecht, The Netherlands.
20. Markley, J. L., Northrop, D. B., and Royer, C. (1996) *High-Pressure Effects in Molecular Biophysics and Enzymology*, Oxford University Press, New York.
21. Holzapfel, W. B., and Isaacs, N. (1997) *High-Pressure Techniques in Chemistry and Physics*, Oxford University Press, Oxford, U.K.
22. Silva, J. L., Foguel, D., and Royer, C. A. (2001) *Trends Biochem. Sci. 26*, 612−618.
23. Panda, M., Ybarra, J., and Horowitz, P. M. (2001) *J. Biol. Chem. 276*, 6253−6259.
24. Gorovits, B. M., Raman, C. S., and Horowitz, P. M. (1995) *J. Biol. Chem. 270*, 2061−2066.
25. Panda, M., and Horowitz, P. M. (2002) *Biochemistry 41*, 1869−1876.
26. Horwich, A. L., Low, K. B., Fenton, W. A., Hirshfield, I. N., and Furtak, K. (1993) *Cell 74*, 909−917.
27. Fayet, O., Ziegelhoffer, T., and Georgopoulos, C. (1989) *J. Bacteriol. 171*, 1379−1385.
28. Cheng, M. Y., Hartl, F. U., Martin, J., Pollock, R. A., Kalousek, F., Neupert, W., Hallberg, E. M., Hallberg, R. L., and Horwich, A. L. (1989) *Nature 337*, 620−625.
29. Braig, K., Otwinowski, Z., Hegde, R., Boisvert, D. C., Joachimiak, A., Horwich, A. L., and Sigler, P. B. (1994) *Nature 371*, 578−586.
30. Braig, K., Adams, P. D., and Brunger, A. T. (1995) *Nat. Struct. Biol. 2*, 1083−1094.
31. Boisvert, D. C., Wang, J., Otwinowski, Z., Horwich, A. L., and Sigler, P. B. (1996) *Nat. Struct. Biol. 3*, 170−177.
32. Xu, Z., Horwich, A. L., and Sigler, P. B. (1997) *Nature 388*, 741−750.
33. Lorimer, G. (1997) *Nature 388*, 720−721.
34. Xu, Z., and Sigler, P. B. (1998) *J. Struct. Biol. 124*, 129−141.
35. Thirumalai, D., and Lorimer, G. H. (2001) *Annu. Rev. Biophys. Biomol. Struct. 30*, 245−269.
36. Grallert, H., and Buchner, J. (2001) *J. Struct. Biol. 135*, 95−103.
37. Saibil, H. R., Horwich, A. L., and Fenton, W. A. (2002) *Allostery and Substrate Conformational Change During GroEL/GroES-Mediated Protein Folding*, Vol. 59, Academic Press, New York.
38. Buchner, J., Schmidt, M., Fuchs, M., Jaenicke, R., Rudolph, R., Schmid, F. X., and Kiefhaber, T. (1991) *Biochemistry 30*, 1586−1591.
39. Goloubinoff, P., Christeller, J. T., Gatenby, A. A., and Lorimer, G. H. (1989) *Nature 342*, 884−889.
40. Laminet, A. A., Ziegelhoffer, T., Georgopoulos, C., and Pluckthun, A. (1990) *EMBO J. 9*, 2315−2319.
41. Martin, J., Langer, T., Boteva, R., Schramel, A., Horwich, A. L., and Hartl, F. U. (1991) *Nature 352*, 36−42.
42. Viitanen, P. V., Lubben, T. H., Reed, J., Goloubinoff, P., O'Keefe, D. P., and Lorimer, G. H. (1990) *Biochemistry 29*, 5665−5671.
43. Horovitz, A., Bochkareva, E. S., Kovalenko, O., and Girshovich, A. S. (1993) *J. Mol. Biol. 231*, 58−64.
44. Todd, M. J., Viitanen, P. V., and Lorimer, G. H. (1994) *Science 265*, 659−666.
45. Yifrach, O., and Horovitz, A. (2000) *Proc. Natl. Acad. Sci. U.S.A. 97*, 1521−1524.
46. Gorovits, B., Raman, C. S., and Horowitz, P. M. (1995) *J. Biol. Chem. 270*, 2061−2066.
47. Weissman, J. S., Hohl, C. M., Kovalenko, O., Kashi, Y., Chen, S., Braig, K., Saibil, H. R., Fenton, W. A., and Horwich, A. L. (1995) *Cell 83*, 577−587.
48. Horwich, A. L., Burston, S. G., Rye, H. S., Weissman, J. S., and Fenton, W. A. (1998) *Methods Enzymol. 290*, 141−146.
49. Holzinger, J., Heumann, H., Manakova, E., Rossle, M., Vanatalu, K., Wiedenmann, A., and May, R. P. (2000) *Physica B 276−278*, 528−529.
50. Weissman, J. S., Rye, H. S., Fenton, W. A., Beechem, J. M., and Horwich, A. L. (1996) *Cell 84*, 481−490.
51. Hayer-Hartl, M. K., Weber, F., and Hartl, F. U. (1996) *EMBO J. 15*, 6111−6121.
52. Llorca, O., Perez-Perez, J., Carrascosa, J. L., Galan, A., Muga, A., and Valpuesta, J. M. (1997) *J. Biol. Chem. 272*, 32925−32932.
53. Clark, A. C., Karon, B. S., and Frieden, C. (1999) *Protein Sci. 8*, 2166−2176.
54. Clark, A. C., Hugo, E., and Frieden, C. (1996) *Biochemistry 35*, 5893−5901.
55. Neuman, R. C., Jr., Kauzman, W., and Zipp, A. (1973) *J. Phys. Chem. 77*, 2687−2691.
56. Ybarra, J., and Horowitz, P. M. (1995) *J. Biol. Chem. 270*, 22113−22115.
57. Yifrach, O., and Horovitz, A. (1995) *Biochemistry 34*, 5303−5308.
58. Burston, S. G., Ranson, N. A., and Clarke, A. R. (1995) *J. Mol. Biol. 249*, 138−152.
59. Rye, H. S., Burston, S. G., Fenton, W. A., Beechem, J. M., Xu, Z., Sigler, P. B., and Horwich, A. L. (1997) *Nature 388*, 792−798.

BI020366J